An Approach Based on Multiobjective Genetic Algorithms to Schedule Observations in Planetary Remote Sensing Missions

Stefano Paterna, *Student Member, IEEE*, Massimo Santoni, and Lorenzo Bruzzone, *Fellow, IEEE*

***Abstract*—Data acquisition in planetary remote sensing missions is influenced by complex environmental resource- and instrument-specific constraints. This impedes to perform observations at any given time during the mission and with any of the instruments composing the scientific payload. This article presents an approach to automatic scheduling of acquisition operations of a remote sensing instrument composing the scientific payload of a mission. The methodology first subdivides the long available observation time intervals into shorter segments and then performs a selection of them, producing an acquisition schedule, optimized with respect to scientific requirements, instrument characteristics, and mission constraints. The scheduling problem is modeled as a multiobjective optimization problem and solved by using Genetic Algorithms (GAs). GAs are able to efficiently explore the solution space by considering different competing objective functions, reaching high-quality solutions. These solutions represent different optimized tradeoffs among the considered instrument-specific quality metrics. The approach is demonstrated on the operations of Radar for Icy Moons Exploration (RIME), a radar sounder onboard Jupiter Icy Moons Explorer. The obtained results show a high potential of the proposed methodology.**

***Index Terms*—Genetic algorithms (GAs), mission operation scheduling, multiobjective optimization, planetary remote sensing, radar.**

I. Introduction

REMOTE sensing instruments provide high-valuable data, characterizing the surface, composition, and structure of the analyzed celestial body. This is possible by exploiting the data acquired by the science payload designed for the considered mission and the related spacecraft. The science payload is usually composed of different instruments, each one devoted to the analysis of a particular variable (or a set of variables) of the considered environment. This often results in a challenging handling of the data acquisition strategy. Indeed, the management of acquisitions requires to consider a large number of complex constraints and specifications. These include scientific objectives associated with each instrument and related requirements, environmental conditions that may limit observation capabilities of certain types of sensors, and resources that are available on board the spacecraft (e.g., power, memory storage space, and downlink data rate) that have to be shared among all the instruments composing the payload. In general, the resources available for a mission and the trajectory to be followed by the spacecraft in the different phases of the mission are defined on the basis of science objectives and related operational requirements of the payload in the early stages of the mission design. Nonetheless, technological issues and cost boundaries limit the resources available to every single instrument. This results in constraints on both the total acquisition time allowed to each instrument and the time distribution of the acquisitions, with the risk to affect the mission science return.

In this context, one of the most important phases of the mission is the scheduling of operations of the science payload. It is aimed at determining the possible options for data acquisitions with respect to the aforementioned constraints. A very important input to this phase is the planned mission trajectory that defines and characterizes the feasible observation opportunities of a certain sensor over a well-defined portion of the target body.

The planning and scheduling phase is, therefore, aimed to produce a scientific payload operations schedule, over a well-defined time frame, which is feasible with respect to both global limitations and the constraints concerning the acquisitions of single sensors. This schedule should optimize the performances of different instruments in terms of data acquisition quality, resource consumption, and compliance to scientific requirements. In particular, for missions that comprehend orbital phases, this means that during the planning and scheduling process, it is mandatory to select a subset of the many available observation opportunities. The selection has to be based on a set of metrics that express the quality of data collection operations performed in each specific time window and in the whole considered time frame.

In the general context of data acquisition planning and scheduling for planetary exploration missions, typical planning procedures are described in [1] and [2]. The process is usually quite long and complex and requires multiple iterations (or cycles) to progressively increase the level of detail of the planning and finally converge to an overall schedule. During these cycles, the instrument teams provide inputs in terms of acquisition requirements and constraints to a mission planning team, which is in charge of collecting the inputs and define the

Manuscript received March 31, 2020; revised June 13, 2020; accepted August 3, 2020. Date of publication August 10, 2020; date of current version August 26, 2020. This work was supported by the Italian Space Agency in the framework of "Attività Scientifiche per JUICE fase C/D" under Grant 2018-25-HH.0. *(Corresponding author: Lorenzo Bruzzone.)*

The authors are with the Department of Information Engineering and Computer Science, University of Trento, I-38050 Trento, Italy (e-mail: stefano.paterna@unitn.it; massimo.santoni@unitn.it; lorenzo.bruzzone@ing.unitn.it).

Digital Object Identifier 10.1109/JSTARS.2020.3015284

acquisition scenarios for the whole scientific payload. Both the overall schedule and the requests from the instrument teams are iteratively refined during the whole process. Thus, the planning phase requires a high percentage of human interaction in the definition of science operation schedules, even if tools such as MAPPS or SciBox (described more in detail in the next section) are available, which can support the following:

1) the definition of the observation strategy;
2) the constraint checking phase; and
3) the translation of the schedules into command sequences to be executed by the spacecraft and its payload.

Further steps toward the development of automatic methods for the planning and scheduling process have been done on Earth observation (EO) missions, which, however, are significantly different from planetary missions in terms of both constraints and scale of the problem. These methods, as we will show in Section II, can be used as an inspiration for addressing the challenges of planetary missions under the assumption of major adaptation and refinements.

In this article, we propose an approach to automatic observation planning and scheduling based on multiobjective Genetic Algorithms (GAs) to be used in complex planetary remote sensing missions. The main goal of the proposed approach is to provide a tool being able to speed up the usually time-consuming observation scheduling process for planetary missions by automatically generating optimal (or nearly optimal) schedules, considering all the mission- and instrument-specific constraints. The proposed technique consists of two main stages, i.e., segmentation and selection stages, during which all feasible acquisition intervals (with respect to the capabilities of the considered instrument) are determined, analyzed, and evaluated to generate the observation sequence for a given sensor over the input time horizon. The segmentation splits the input time horizon into well-defined shorter acquisition intervals, following a time-based or target-based criterion (namely, the start and end times of the interval are determined as the window in which the whole considered target is visible). In the selection phase, an NSGA-II-based engine explores the space of solutions related to the combinations of acquisition segments, by analyzing different objectives expressed by competing metrics. Two slightly modified versions of NSGA-II [3] have been considered: one exploits the mission constraints so that no unfeasible solutions can be generated and evaluated to minimize the computational time; the other implements a local search strategy to better guide the solution space exploration. At convergence, the system provides operation schedules that are optimized (in the Pareto front sense) with respect to different objectives such as data acquisition quality, resource consumption, and compliance to scientific requirements. To validate our approach, we studied the real case of operation planning and scheduling for the JUpiter Icy Moons Explorer (JUICE) mission of the European Space Agency (ESA), which is focused on the analysis of the Jovian System and of Jupiter's Icy Moons. In detail, we focused our attention on the observations of the Radar for Icy Moons Exploration (RIME), the radar sounder designed for JUICE.

The rest of this article is organized as follows. Section II provides an overview on the state-of-the-art on planning and scheduling tools and algorithms exploited for planetary exploration and EO missions. Section III illustrates the proposed methodology in general considering neither any specific instrument nor any specific mission. Section IV illustrates how the proposed methodology can be applied to the case of radar sounder acquisitions. Section V presents the application of the proposed methodology to RIME in the context of the JUICE mission, the experimental setup, the specific choices in terms of constraints and objective functions, and the results are shown and discussed. Finally, Section VI concludes this article.

II. State of the Art

In this section, we present methodologies that are currently exploited to solve the problem of planning and scheduling of science operations for planetary exploration missions. Moreover, we present methods and tools devoted to the automatic creation of schedules for EO missions, which can be used as an inspiration for planetary exploration missions.

A. Planning and Scheduling in Planetary Missions

As explained in [1] and briefly addressed in Section I, the planning process takes place over different cycles that have different length and also different levels of detail. They are usually divided in the following.

1) *Long-term planning cycle*: The first planning cycle is devoted to both the analysis of the overall objectives of the mission (given the spacecraft trajectories) and their feasibility with respect to the general and instrument-specific constraints. It allows us to define observation opportunities for each instrument and also to determine a preliminary profile of observation plans from the point of view of required resources and of the quality of observations.
2) *Medium-term planning cycle*: The second planning cycle is usually shorter and has the goal to define the required resources in more detail and to allocate them to each experiment.
3) *Short-term planning cycle*: The final cycle is devoted to the high detail planning of science activities and to the definition of operational command sequences to be executed to realize them.

Tools such as MAPPS [1] or SciBox [2] are usually exploited especially to aid the medium- and short-term planning cycles. Their main feature is the capability to take as input a set of mission- and instrument-specific constraints (e.g., the instrument pointing) and objectives, together with spacecraft trajectory information and preliminary operation schedules, and to provide as output a visualization and a manually modifiable schedule, in which constraint violations are pointed out. Moreover, they can transform the set of scheduled science operations into command sequences and activities that have to be executed to perform the observation. MAPPS is able to simulate input schedules, providing a detailed profile of resource consumption versus time caused by scheduled science operations. Moreover, it provides 2-D projection maps, showing geometric features of the observations and the associated data with respect to the target body surface (i.e., the projection of the instrument field

of view on a surface map). SciBox provides similar visualization capabilities, but it also implements an automatic schedule building tool. Once all observation opportunities related to determined objectives and their characteristics are defined, these observations are ranked on the basis of related quality metrics (e.g., illumination of the scene and resolution of the collected data), which can be extracted from the spacecraft trajectory and pointing information. Observations are added to the schedule based on their rank until any constraint gets violated.

A further tool, similar to MAPPS and SciBox, is MAPGEN [4], developed at the NASA Ames Research Center and the Jet Propulsion Laboratory. Like the two engines mentioned above, MAPGEN provides the user with timeline visualization capabilities and is able to produce feasible schedules of top-level science operations in planetary missions. Thanks to the APGEN engine, top-level operations defined by the user are translated into lower-level activities based on an activity dictionary. This enables a thorough analysis of both the operation impact on resource consumption and the constraint compliance. Based on the mission global constraints defined in the planner domain and on further user-defined limitations, MAPGEN is able to generate feasible acquisition strategies that can be further manually modified, thanks to the GUI implemented in the planning tool. MAPGEN requires the user to specify the initial plan state, observation goals, and their priority scores, apart from the aforementioned rules and constraints on the observation sequence construction. In particular, user-specified priorities are exploited in order to solve any constraint violation in the generated schedule, removing partially or totally the observation with lower scores. The tool also offers the opportunity to the user to manually modify the produced schedules, in order to make them more appropriate to their requirements.

B. Planning and Scheduling Methods in EO Missions

The methods developed for EO missions are used in contexts that are often different from those encountered in planetary exploration missions. Indeed, planetary missions require approaches that aid the operation analysis and scheduling process already before the mission launch and consider long time horizons. The automatic scheduling methods designed for EO missions usually work at regular intervals, considering short time windows (usually the analyzed window lasts 24 h), while the mission is ongoing. The main drivers for the acquisition planning, in the EO case, are acquisition requests of well-defined targets, which can be represented either as point targets or as areas of interest (AOIs). Thus, most of the automatic techniques for EO have been developed for the short-term planning and scheduling tasks, in order to build feasible schedules in a fast way. Two very similar approaches to the scheduling problem are presented in [5], regarding the acquisitions with ASTER (on-board NASA's EOS-AM1 satellite), and in [6], regarding the observations to be performed by the synthetic aperture radar on-board DLR's TerraSAR-X satellite. In both cases, acquisition requests identify the regions on Earth that should be observed, called AOIs. These regions are intersected with the swathes determined by observation capabilities of sensing instruments during the orbit of the spacecraft. This intersection defines observation opportunities, associated with determined time intervals, that the scheduling algorithm can select. For both mentioned algorithms, the selection of opportunities is based on a priority score. In [5], observation opportunities are first subdivided into shorter parts, called scenes, each of which is characterized by a score, determined by the quality of the observation over that particular portion of the surface and by the degree of priority of the related acquisition request. The overall priority score for the opportunity is then calculated by summing the scores of all its scenes. In [6], instead, the priority of an opportunity is defined by assigning a score between 0 and 9 to the related acquisition request. The opportunities are ranked based on the priority score. Both algorithms iteratively select the opportunity with the highest priority, assess its resource consumption, and add the opportunity to the schedule. A constraint check is performed, and if any resource constraint is violated by adding the considered acquisition opportunity to the schedule, the opportunity is deleted and will no longer be considered for the following steps. Both methods consider a scheduling time frame of one day, but the algorithm described in [6] is executed every 12 h.

This kind of approach is not appropriate for our analysis, as it generates schedules in a very quick way, but considering only metrics that qualify the single opportunity/data take. This does not guarantee to obtain an overall optimized schedule of the acquisitions in a complex scenario and on a long time frame. Indeed, the number of feasible opportunities that are taken into account is limited on a time frame of 24 h.

Other methods to perform observation scheduling of EO missions consider the use of deterministic optimization methodologies such as the depth-first branch and bound [7]. As in the previously mentioned methods, first, acquisition opportunities among which to perform the selection are identified by intersecting the AOIs with the swathes formed by projecting the field of view of the considered instrument on the Earth surface; then, the target polygons are subdivided into so-called shards, which are subsections of the targets that can be acquired. They can be easily formed by intersecting the edges of swath segments and target polygons. Each of the shards has an associated reward value (which, for example, can be the area covered by the shard), while the segments carry with them the information about their cost (for example, the memory capacity required to store the data associated with that segment). This formulation allows one to update the available capacity depending on the selection or rejection of a segment. The node ordering heuristic, starting from an empty solution, takes a partial solution **R'** and the available segments $s \in \mathbf{R}$ (where **R** includes all the segments associated with their downlink opportunity), $s \notin \mathbf{R'}$, and orders them accordingly. The basic approach is to calculate the reward/cost associated with the inclusion of each set not yet included in the solution. This technique might still not be appropriate for the case we are considering, due to the large dimensions of the problem, since it uses a deterministic optimization algorithm. A more interesting approach is the one presented in [8], where a set of R_{tasks} requested tasks to be performed on the considered day is taken into account.

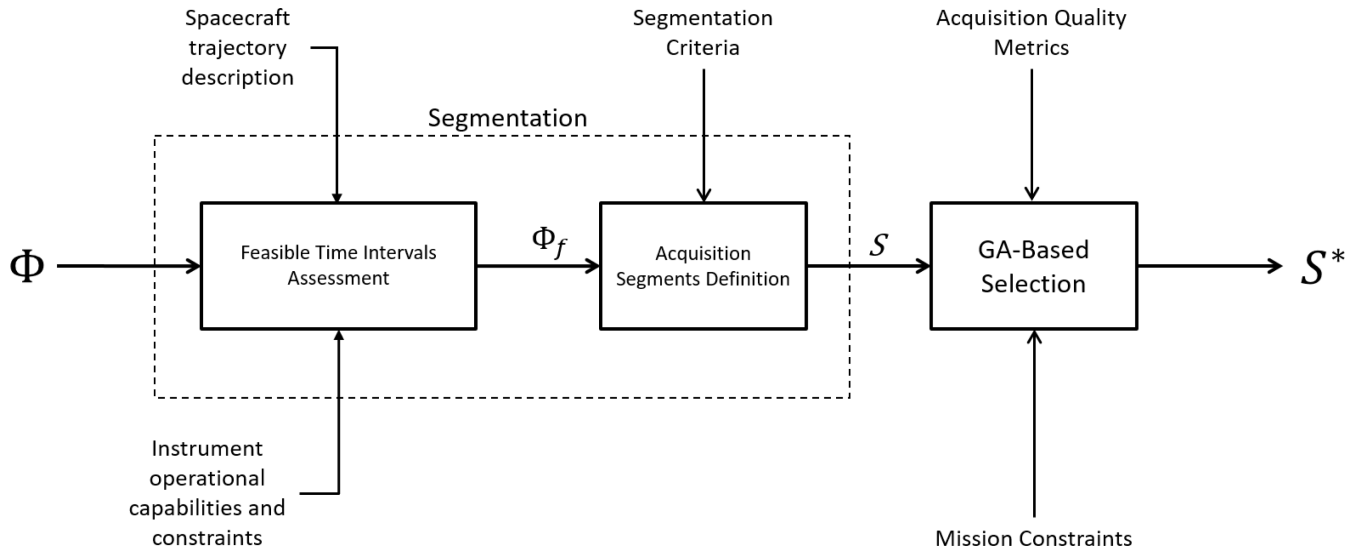

Fig. 1. Illustration of the steps of the proposed methodology: here, Φ represents the total time interval that we are taking into account (i.e., a particular phase of the considered mission) and $\Phi_f \subset \Phi$ is the set of time intervals $\phi_i^f \in \Phi$, in which data acquisition with the specified instrument is feasible. S is the result of the subdivision of Φ_f in shorter time segments $s_i \in S$, which are easier to handle and analyze. Finally, $S^* \subset S$ represents an optimal subset of S with respect to instrument-specific quality metrics and general constraints.

A set of Orb orbits over which the different tasks can be accomplished is examined. Different acquisition opportunities for a single task over the different orbits are identified and described by several metrics that define the energy and memory consumption, but also the required sensor slewing angle. In addition to the metrics, constraints on the cost of performing different data acquisitions are considered: for example, the energy consumption due to the acquisition and the sensor slewing operations over a certain orbit shall not exceed a well-defined amount. A very similar constraint is also expressed regarding the memory consumption over a certain orbit. These metrics are then combined in a parameter that expresses the weight of completing the considered task at a particular orbit. The final goal is to construct the schedule that maximizes the total profit associated with the set of tasks scheduled for the considered day, without violating any constraint. The objective function to be optimized is defined as follows:

$$\max\left\{\sum_{j=1}^{Orb}\sum_{i=1}^{R_{\text{tasks}}} y_{i,j} w_i\right\} \tag{1}$$

where $y_{i,j} \in \{0,1\}$ expresses if the ith task is scheduled to be performed on the jth orbit and the weight w_i expresses the aforementioned combination of metrics describing the score of the acquisition opportunity. The effective selection of the tasks to be scheduled on the considered day is performed using a stochastic optimization algorithm based on simulated annealing. This methodology has the advantage to use a stochastic optimization technique that can solve large-scale problems. Moreover, the way in which the problem is represented can be a very good starting point to describe the problem we are addressing, even if this methodology still considers a quite short time frame of 24 h, like the methods shortly described before.

III. Proposed Planning and Scheduling Approach

The methodology that we propose to automate the planning and scheduling process consists of two main phases (see Fig. 1): *segmentation* and *selection*. The segmentation phase takes as input the whole set of feasible acquisition time intervals (contained in the total considered time interval Φ), splits them into shorter segments, following a user-defined criterion, and extracts a set of significant metrics describing each of the acquisition segments. These metrics are then exploited in the selection phase, in which they are combined in suitable cost/fitness functions that express the acquisition schedule quality. The selection phase is aimed at building an optimized acquisition schedule. This result is obtained by using an optimization algorithm, which efficiently explores the solution space and selects an appropriate subset of acquisition segments, given science and instrument requirements, acquisition quality metrics, and mission constraints. The list of the symbols used hereafter to formalize the proposed methodology is shown in Table I.

A. Segmentation Phase

As shown in Fig. 1, inputs to the whole system are the total considered interval Φ and the description of the trajectory that the spacecraft will follow during its orbit around the target celestial body. The latter is defined using kernel files that contain the state vector (describing position and speed) of the satellite in time, using a format that is the standard *de facto* for the description of trajectories of spacecraft. The interface to these kernel files is provided by dedicated libraries, which allow us to extract all the useful information about the spacecraft motion around the celestial body to be investigated and about the acquisition scenario. Examples of these libraries are the ones created by NASA' s Navigation and Ancillary Information Facility, called SPICE [9], [10]. On the basis of orbit data, it is

TABLE I
LIST OF SYMBOLS (AND THEIR DEFINITION) USED TO DESCRIBE THE PROPOSED METHODOLOGY

Φ	Full considered time interval (i.e., the time span of a particular mission phase).
$\Phi_f = \{\phi_1^f, \phi_2^f, ..., \phi_P^f\}$	Set of time intervals in which the acquisition is feasible with respect to the analyzed instrument capabilities and limitations.
$S = \{s_1, s_2, ..., s_N\}$	Set of the acquisition segments in which Φ_f is subdivided.
s_i	i-th acquisition segment.
$S^* \subset S$	Subset of acquisition segments that constitute the acquisition schedule, resulting from the selection phase.
N	Number of acquisition segments $s \in S$.
$\mathbf{x}$	Vector of the variables (x_i) associated to the acquisition segments and used in the selection phase.
$x_i = x(s_i)$	Binary variable ($x_i \in \{0, 1\}$) associated to the i-th acquisition segment, determining if that segment is included in the acquisition schedule ($x_i = 1$) or not ($x_i = 0$).
$st(s_i)$	Start time of the i-th acquisition segment.
$et(s_i)$	End time of the i-th acquisition segment.
$time(s_i)$	Duration of the i-th acquisition segment.
$day(s_i)$	Day in which the acquisition identified by s_i would take place.
$a(s_i)$	Area covered by the i-th acquisition segment.
$e(s_i)$	Energy consumption associated to the data acquisition operation performed from $st(s_i)$ to $et(s_i)$.
$m(s_i)$	Storage memory consumption associated to the data acquisition operation performed from $st(s_i)$ to $et(s_i)$.
En	Available energy on board the spacecraft.
Mem	Available storage memory on board the spacecraft.
$dat_d(\mathbf{x})$	Acquisition time associated to day d, given the candidate schedule expressed by $\mathbf{x}$.
$\mathbf{g}_d = \{g_{d,1}, g_{d,2}, ..., g_{d,N}\}$	Vector used as support to define $dat_d(\mathbf{x})$.
$g_{d,i} = \{0, 1\}$	Component of $\mathbf{g}_d$.
A	Total surface to be covered with the acquisitions performed by the considered instrument.
A_s	Surface covered by the acquisition segments included in the considered schedule.
A_o	Total overlap surface of the influence areas $a(s_i)$ associated to the segments included in the considered schedule.
$t(s_i)$	Metric to support the proposed mutation operator, expressing how well adding the segment s_i to the considered solution improves the total coverage.
$r(s_i)$	Metric to support the proposed mutation operator, expressing how well removing the segment s_i from the considered solution reduces the coverage overlap.
q_i	Generic quality metric of the observation associated to the segment s_i.

possible to perform a first filtering of time intervals, removing all the time intervals in which acquisitions with the analyzed instrument are not feasible due to the characteristics of the instrument with respect to environmental conditions (e.g., an optical camera can only acquire images on the illuminated side of the considered celestial body) and to other mission-related limitations that might prevent any instrument from performing acquisitions. This filtering can be done by exploiting dedicated function libraries (e.g., SPICE) mentioned above. Indeed, using

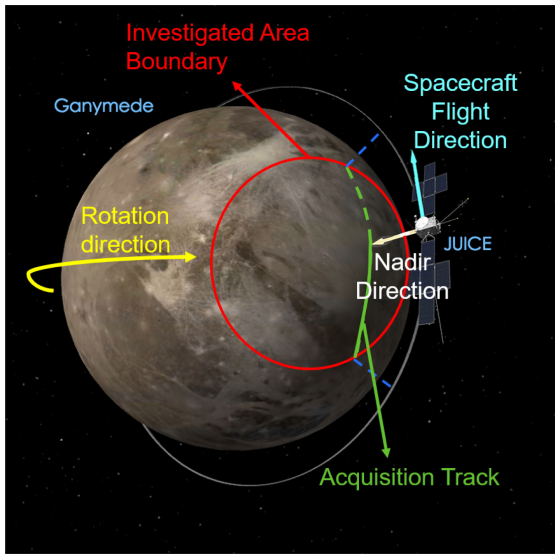

Fig. 2. RIME acquisition scenario at Ganymede. The red circular area defines the portion of the surface, in which acquisitions with the radar sounder RIME are not affected by Jupiter radio emissions.

those conditions and limitations as input to these functions, it is possible to easily recognize the time intervals in which they are verified and remove them from the time horizon Φ. After this filtering phase that produces the set Φ_f of time intervals in which the acquisition operations of the considered instrument are feasible, the next step is to determine the area that we can observe at each time instant. If we consider an instrument with fixed pointing, this is possible by simply projecting the position of the spacecraft on the surface of the target body along the pointing direction. Fig. 2 shows how this operation is performed for the case of the radar sounder RIME, which is the study case we consider in this work (see Section V for more details).

The resulting opportunities and the ground tracks related to time intervals Φ_f are often too long to be acquired in a single continuous observation. Therefore, the successive step is to subdivide them into shorter acquisition segments s, which can be more easily managed during the mission operation. We can define these segments as single uninterrupted time intervals, in which different desired conditions are verified. These conditions for the segmentation should be given as input to the framework, as shown in Fig. 1. An easy condition, following which we might want to subdivide the long acquisition time intervals in Φ_f, could be the duration, therefore creating a set of segments with equal or similar time span. Moreover, once the pointing of the instrument is fixed (also the information regarding the pointing is contained in the kernel files), it is straightforward to translate the time instants in Φ_f into observable positions on the target's surface (expressed as latitude and longitude coordinates). Thus, it is possible to perform the segmentation directly on the related ground tracks to take into account high-interest areas on the target body's surface. Indeed, it is convenient to perform acquisitions over these important areas in a continuous way, to ease the interpretation and the extraction of information from the acquired data. After the identification of these high-interest

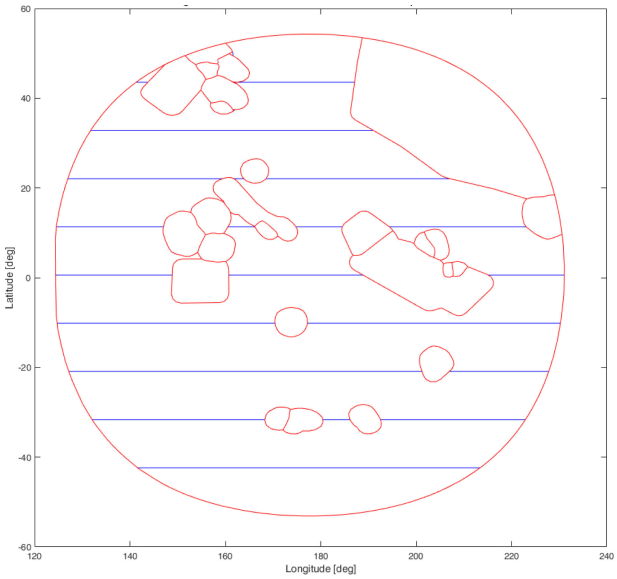

Fig. 3. Example of segmentation grid of the "operative" zone for the orbital phase at 500-km altitude around Ganymede (GCO-500) of the JUICE mission. The borders of the higher relevance areas are shown in red, while the rest of the surface is subdivided in latitude bands (in blue). This grid is used to segment the whole set acquisition opportunities, once their relative position on Ganymede's surface has been determined.

areas and the determination of their coordinates, the remaining portion of the surface to be observed can be further subdivided in a uniform way. Thus, we can create a particular mapping of the analyzed celestial body surface that we call a *segmentation grid*. Fig. 3 shows an example of a segmentation grid as applied to the test case described in Section V. The single areas in which the surface to be observed is subdivided (both the target areas and the other remaining surface portions) are called *cells*, and the long acquisition tracks are split at the edges of them. Therefore, in this case, the conditions to be verified are spatial: we define the acquisition segments as the individual time intervals in which the observable portion of the surface is delimited by a particular cell. Thus, the start and end times of each segment are determined as the time instants in which the observable portion of the surface crosses the border of one of the cells.

The output of the segmentation stage is a set of acquisition segments $S = \{s_1, s_2, \ldots s_N\}$, where N is the total number of resulting segments.

These acquisition segments are then described by a set of metrics. The most important and general segment metrics are as follows.

1) $st(s_i)$ and $et(s_i)$ identify the beginning and the end of the acquisition segment s_i from the temporal point of view. They are defined as a result of the temporal or spatial segmentation described above.
2) $time(s_i) = et(s_i) - st(s_i)$ is derived from the previous metrics and determines the temporal duration of segment s_i.
3) $a(s_i)$ is the portion of surface covered by segment s_i. It is obtained by splitting the projection of the instrument field of view on the surface in correspondence of the spatial coordinates between the instants $st(s_i)$ and $et(s_i)$.

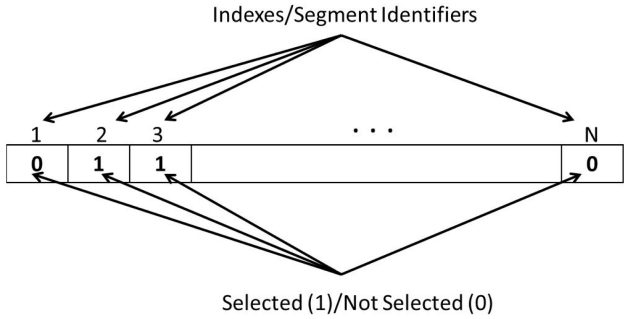

Fig. 4. Illustration of the radar sounder acquisition geometry (figure taken from [18]). Radar sounders are nadir-pointing instruments. They produce tomographies of subsurface features (B), below the regions identified in the figure as ground tracks (A), exploiting the platform movement. Points C and D are off-nadir sources of nondesired echoes, which might interfere with the characterization of subsurface features placed long the nadir direction.

4) $e(s_i)$ and $m(s_i)$ represent the energy and the memory consumption associated with the acquisition operation of segment s_i, respectively. They are defined on the basis of the characteristics of the instrument in terms of energy and memory consumption rates.

Further metrics to describe the acquisition segment could be specifically created and extracted, based on the characteristics of the considered instrument, of the analyzed mission, and of the environment in which the instrument should operate.

B. Selection Phase

Following the definition of the metrics that describe each acquisition segment and the whole acquisition strategy (based on the segment metrics), in the selection phase, the subset S^* of segments that satisfies scientific requirements in the best possible way should be selected without violating any constraint. We can represent a possible schedule as a binary vector $\mathbf{x}$ ($\mathbf{x} = \{x_1, x_2, \ldots, x_N\}$), in which every position i identifies one of the acquisition segments s_i, and the value x_i ($x_i \in \{0, 1\}$) of the ith position of the solution vector $\mathbf{x}$ expresses if that particular acquisition is inserted in the schedule (1) or not (0) as represented in Fig. 4. This is a combinatorial problem that can be modeled as a particular type of multidimensional 0–1 knapsack problem [8]. Multidimensional knapsack problems [11] are a very good example of a combinatorial problem, in which the objective is to maximize a total profit parameter associated with a subset of the available objects, given a set of constraints based on cost coefficients associated with these objects. Each of these objects has associated a profit coefficient and cost coefficients that depend on different constraints.

In general, different metrics to be optimized can be considered simultaneously. However, often these metrics express objectives that might be conflicting between each other. Accordingly, in the proposed approach, we address this issue by exploiting a multiobjective optimization approach.

The result of such optimization is a set of different solutions that represent the Pareto front, i.e., the set of the nondominated solutions [12]. For a multiobjective maximization problem, a given solution $\mathbf{x}_1$ of the optimization problem dominates another solution $\mathbf{x}_2$ if $f_j(\mathbf{x}_1) \geq f_j(\mathbf{x}_2)\,(\forall j = 1, 2, \ldots, O)$ and $f_k(\mathbf{x}_1) >$

$f_k(\mathbf{x}_2)$ at least for one objective $f_k(\mathbf{x})$ $(k = 1, 2, \ldots, O)$ [13], where $f_j(\mathbf{x})$ and $f_k(\mathbf{x})$ are different objectives that are taken into account and O is the total number of analyzed objectives. It is worth noting that a single-objective approach cannot ensure the control on all the metrics that describe the quality of the acquisition campaign, even if we combine different quality metrics in one single cost/objective function. The multiobjective approach, instead, has the advantage of producing solutions that represent multiple optimal tradeoffs between different objectives. In the case of the segment selection problem, this results in a set of optimal acquisition schedules, which are all nondominated solutions with respect to the considered quality metrics. Thus, any of these solutions could potentially be selected as the final observation schedule for the considered instrument. The final choice is only guided by the desired tradeoff between the selected quality factors. Moreover, since we are taking into account acquisition operations of a single instrument in missions that usually have a large scientific payload, having different optimal solutions with different tradeoffs can be very useful to choose the strategy that better adapts to the acquisition requirements and schedules of other instruments.

Let $\mathbf{x} = \{x_1, x_2, \ldots, x_N\}$ be the vector of the decision variables, $F(\mathbf{x}) = \{f_1(\mathbf{x}), \ldots, f_l(\mathbf{x}), \ldots, f_O(\mathbf{x})\}$ be the set of objectives/fitness functions that are related to the quality metrics we need to optimize, $f_l(\mathbf{x}) \in F$ be one of the functions indicating the quality of the schedule identified by $\mathbf{x}$, and q_i be a generic quality metric associated to the segment s_i. In the case we are analyzing, a possible quality metric q_i could be the parameter $a(s_i)$. We formulate the segment selection problem as follows:

$$\max_{\mathbf{x}} \{F(\mathbf{x})\} \tag{2}$$

$$\text{with } f_l(\mathbf{x}) = \sum_{i=1}^{N} q_i x_i \tag{3}$$

$$\text{subject to} \sum_{i=1}^{N} c_{j,i} x_i < b_j, \quad j = 1, \ldots, M \tag{4}$$

$$x_i \in \{0, 1\}, \quad i = 1, \ldots, N. \tag{5}$$

The cost coefficient $c_{j,i}$ $(j = 1, 2, \ldots, M, i = 1, 2, \ldots, N)$ is associated with the jth constraint and to the ith position of the solution vector (i.e., to the ith acquisition segment s_i). The parameter b_j is a component of the vector $\mathbf{b}$ $(\mathbf{b} = \{b_1, b_2, \ldots, b_M\})$, which contains the values of the bounds associated with each of the M constraints. Moreover, we have a set of multiple global constraints that should guide us in the selection of the correct subset of segments also based on their associated metrics. The global quality function $f(\mathbf{x})$ can, in general, be more complex than the one shown in (3), but that formulation is a good representation for many acquisition schedule quality metrics.

In order to solve this kind of problem, given that in general the number of acquisition segments is very high, we use stochastic optimization techniques that can explore the solution space in an efficient way, without the need to explicitly evaluate the whole set of possible combinations of acquisition segments. A suitable option is to use a technique based on GAs, which have been used in a variety of applications (i.e., [14]), providing very good results.

GAs have also been applied to specific satellite scheduling problems, for scheduling the downlink from the satellite to a ground station, given the visibility intervals and the possible ground stations on Earth [15], [16]. Note that the structure used to represent the different solutions in GAs, the *chromosome*, is intrinsically suitable to the representation of our problem in form of a binary vector. Another important property of GAs is that genetic operators, crossover and mutation, allow for a good exploration of the solution space by generating new solutions combining the current ones or slightly modifying a small number of variables of them. In general, the mutation operator randomly modifies one or more of the components x_i of the solution vector $\mathbf{x}$ to a certain extent; in the case of a binary solution vector, it simply changes the value of x_i from 0 to 1 or from 1 to 0. In our case, this results in adding the related segment s_i to the schedule we are building, or removing s_i from it, respectively. The crossover operator instead produces new solutions considering input pairs of solution vectors of the previous iteration. It subdivides input solution vectors into two or more components in correspondence with the crossover points. Considering to have one crossover point, two new solution vectors are generated. The first solution is made by joining the first component of the first input solution vector and the second component of the second input solution vector. The first component of the second input solution vector and the second component of the first input solution vector constitute the second new solution generated by crossover.

Since we formulated the acquisition segment selection as a multiobjective optimization problem, a suitable algorithm to solve it is NSGA-II [3], which is one of the most effective multiobjective versions of GAs. The algorithm is initialized either with a randomly generated or with a custom population of candidate schedules, modeled as binary vectors. At iteration h, for each member of the current population Pop_h, the values of all the cost/objective functions are computed. The members of Pop_h are sorted following the nondomination criterion based on the values of the considered quality metrics, assigning a rank to each member based on its nondomination front (or level). A further metric controlling the density of the population members in the objective function space (which is the crowding distance) is also computed for each candidate acquisition schedule in Pop_h. The offsprings (new candidate schedules) O_h are created by selecting members from Pop_h via binary tournament selection and using them as input to the crossover and mutation functions. The binary tournament selection is based on the rank (the lower, the better) and in case two members with same rank are picked, the one with larger crowding distance will be selected, to ensure that the final solutions of the optimization will be well distributed along the Pareto front. Moreover, NSGA-II implements the concept of elitism: indeed, in order to create Pop_{h+1}, the offsprings O_h are considered together with the members of Pop_h. The members of $Pop_h \cup O_h$ are ranked following the nondomination criterion, after the evaluation of the objective functions for the members of O_h. Pop_{h+1} is created by picking the best $|Pop_h|$ candidate schedules from $Pop_h \cup O_h$ based on their rank (nondomination

level) and using the crowding distance as a tie-breaker to decide between candidate solutions with the same rank.

However, given the dimension of the problem, NSGA-II would not be able to easily converge to a good set of solutions close to the Pareto front, despite the potentialities given by its features. Thus, we need to modify the algorithm, implementing hybrid strategies to improve the way in which we explore the solution space. A possible strategy is to modify the way in which new candidate solutions are generated, implementing constraints inside the evolutionary operators (crossover and mutation), so that only feasible solutions are generated. In general, constraints can be represented in matricial representation as

$$C\mathbf{x} < \mathbf{b} \tag{6}$$

where $C \in \mathbb{R}^{M \times N}$ is the matrix that represents all the cost coefficients associated with each variable of the solution vector $\mathbf{x}$ and each constraint that we need to apply (e.g., energy, memory, and time). The cost coefficient $c_{j,i}$ defined above represents the generic component of the matrix C. The constraints that can be introduced in the scheduling process should be carefully designed, depending on the characteristics of the mission, of the considered instrument, and of the acquisition environment. However, as an example of constraint that could be useful in general, we can use the segment metric $m(s_i)$ that has been described in the previous section, regarding the memory consumption. We can define the vector $\mathbf{c}_j$ (being $\mathbf{c}_j$ a row of the matrix C) as

$$c_{j,i} = m(s_i) \tag{7}$$

and formulate the constraint as

$$\sum_{i=1}^{N} c_{j,i} x_i < Mem \tag{8}$$

where Mem identifies the amount of storage memory that is available between two consecutive downlink windows and thus the amount of data that can be downlinked in a specific downlink window. We can easily associate each segment s_i to the downlink window, in which the data volume generated between $st(s_i)$ and $et(s_i)$ ($m(s_i)$) is effectively transmitted to the ground station. Thus, given this association, the constraints on the memory consumption can be defined for each downlink window, considering only the segments related to the specific downlink window. This allows us to better control the state of the memory storage on board the spacecraft throughout the whole considered time frame. This formulation is inserted in the genetic operators, in order to check the generated solutions and, if any constraint violation is detected, to correct the nonfeasible solutions changing the value of some of the associated variables from 0 to 1 or from 1 to 0, accordingly. This introduces a first limitation on the exploration of the solution space.

Another possibility to increase the efficiency of the exploration is to further modify the mutation operator in order to perform a smarter exploration of the solution space. The operator should modify the input solution vectors such that this modification is guided toward solutions that are better from the point of view of the specified objectives.

This should be done by exploiting our knowledge of the problem and the characteristics of each segment $s_i \in S$. In particular, inspired by the local search strategy proposed in [17], by maintaining the randomness of the GA, a higher weight (and therefore a higher probability to be selected) can be given to the variables/segments that improve the considered solution/schedule if added or removed from it. Based on the metrics that can be extracted for each acquisition segment, further metrics can be calculated based on the scenario represented by the input solution vector. More in detail, we can identify the following three possible actions:

1) adding segments to the schedule;
2) removing segments from the schedule; and
3) replacing a segment in the schedule (a mixture of the previous two actions).

For modeling this last case, it is useful to define two additional sets of segments.

1) $S_{\text{in}} = \{s_i \in S : x_i = 1\}$, which is the set of segments included in the input schedule/solution vector.
2) $S_{\text{out}} = \{s_i \in S : x_i = 0\}$, which is the set of segments not included in the input schedule.

Initially, the action to be performed is randomly selected. Given the action to perform, one should focus either on S_{in} (for the removal action) or on S_{out} (for the addition action) and compute metrics that guide the search toward better solutions. These metrics are then used in order to implement a *roulette wheel selection* mechanism, to decide which segments should be added, removed, or substituted to improve the characteristics of the input observation schedule. For example, in our case, we can extract the information regarding the area $a(s_i)$ covered by each acquisition segment. Considering an acquisition schedule modeled as the binary vector $\mathbf{x}$ as input to the modified mutation operator, if the selected action is to add a segment to the schedule, the goal can be to increase the total surface covered by the segments $s_i \in S_{\text{in}}$. We can define A as the total surface that has to be covered and A_s as the surface covered by the current solution

$$A_s = \bigcup_i \{a(s_i) : s_i \in S_{\text{in}}\}. \tag{9}$$

We can, therefore, define for each $s_j \in S_{\text{out}}$ a metric of "surface improvement" as follows:

$$t(s_j) = a(s_j) \cap (A - A_s) \quad \forall s_j \in S_{\text{out}}. \tag{10}$$

The higher the value of $t(s_j)$, the higher the probability of s_j to be included in the output schedule. The values of $t(s_j)$ are calculated for each of the segments in S_{out} and then used to pick the segments to be added to the output acquisition schedule. A similar situation happens if the selected action is to remove segments from the input schedule: in this case, the goal might be to reduce the overlapping between all the $a(s_i)$ with $s_i \in S_{\text{in}}$. For this case, we can, therefore, define the total overlap area A_o as

$$A_o = \bigcup_{i,j} \{a(s_i) \cap a(s_j) : i \neq j, s_i, s_j \in S_{\text{in}}\}. \tag{11}$$

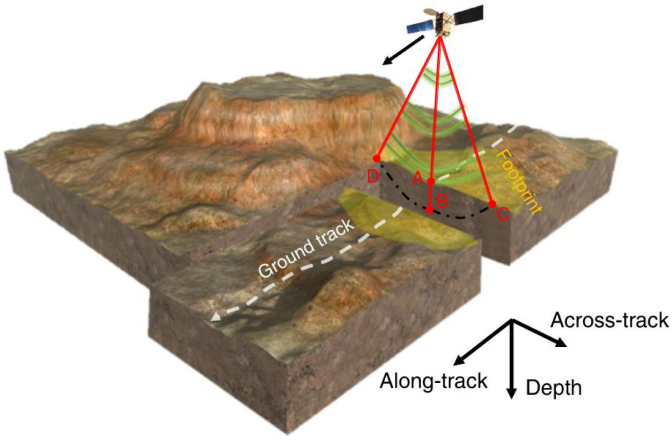

Fig. 5. Binary vector representation of the scheduling problem in the phase of selection of acquisition segments.

We can, therefore, define for each $s_i \in S_{\text{out}}$ a metric of "overlap reduction" as follows:

$$r(s_i) = a(s_i) \cap A_o \quad \forall s_i \in S_{\text{in}}. \tag{12}$$

Again, the higher the value of $r(s_i)$, the higher the probability of s_i to be excluded from the output schedule. The values of $r(s_i)$ are calculated for each of the segments in S_{in} and used to pick the segments to be removed from the output acquisition schedule. Further details on how this modified mutation operator is used and on the metrics that have been exploited are given in Section V.

IV. Proposed Approach: Application to Radar Sounder Acquisitions

In this article, we apply the proposed approach to the study of acquisition operations of a radar sounder, defining metrics to describe the quality of the related acquisition campaign. Many planetary missions include radar sounder systems in their scientific payloads, such as MARSIS (instrument on ESA's Mars Express [19]) and SHARAD (on the NASA's Mars Reconnaissance Orbiter [20]). Radar sounders have a particular acquisition geometry and specific observation capabilities, as illustrated in Fig. 5. They are nadir-looking pulsed radars that are able to penetrate the ground and, therefore, to perform direct measurements on the shallow subsurface of the observed body, thanks to the relatively low frequency of the electromagnetic pulses that they emit. The characterization of the subsurface's structures is obtained by measuring the reflections caused by interfaces between targets or layers with different dielectric properties and representing them as a radargram. A single radargram represents a vertical profile of the subsurface of the illuminated area on the body's surface. This is obtained by acquiring consecutive columns along the direction of movement of the platform on which the radar is mounted. In the produced image, backscattered signals are mapped on the vertical direction, transforming the information relative to the time interval between the pulse transmission and the signal reception into the distance of the scattering object from the platform. By performing multiple acquisitions on different ground tracks over a certain area on the ground, it is possible to collect a detailed information on the subsurface of the observed body and on the subsurface feature distribution. Usually, acquisitions should be uniformly distributed over the considered celestial body with a given predefined distance between the ground tracks. These tracks are identified by nadir-projecting the position of the satellite in time on the body surface.

A more detailed analysis of the subsurface structure of the investigated celestial body can be done by acquiring data over intersecting ground tracks. These data can be used to perform a 3-D reconstruction of the properties of the subsurface.

We use this kind of instrument for illustrating the use of the proposed approach. In order to define the quality of the acquisition strategy of planetary radar sounders in general, we consider the following variables (also investigated in [21], which provides an analysis on radar sounder observations):

1) the uniformity in space of the data acquisitions, checking how well the requirement in terms of distance between ground tracks is met;
2) the number of intersection points and the position and distribution on the surface;
3) the presence of areas of higher interest, which need higher acquisition track density;
4) the presence, in different zones of the investigated celestial body, of target areas over which acquisitions should be performed uninterruptedly.

Then, in specific missions, additional variables might constrain acquisitions, as described in Section V. The third and fourth variables can be taken into account during the segmentation phase, by applying a spatial segmentation, as described in Section III-A. Regarding the uniformity in space of data acquisitions, this requirement can be considered by slightly modifying the concept of the area $a(s_i)$ covered by the segment s_i, since the instrument does not produce an image of the surface but rather a tomography of the subsurface. $a(s_i)$ can be obtained by enclosing each of the ground tracks related to the acquisition segments s_i in areas that have the same length of the ground tracks and a width equal to the desired distance between tracks. For the radar sounder case, $a(s_i)$ is, therefore, called *influence area*. Thus, using this formulation, we can express the uniformity requirement as a surface "coverage" requirement, similarly to what one can do for other imaging systems, for which $a(s_i)$ can be defined in a more straightforward way considering their imaging capabilities.

V. Experimental Results

As mentioned in Section IV, for validating the proposed approach, we considered the planning and scheduling of the acquisitions of a planetary radar sounder, analyzing a real case. We used as test case the operations of the radar sounder RIME [22], [23] on board the JUICE mission. The JUICE mission, which includes 11 instruments in its scientific payload, is aimed to study the Jovian system. Its main objectives are the analysis of the Icy Moons of Jupiter: Ganymede, Europa, and Callisto.

A. Test Case Considered: RIME and the GCO-500 Phase

In our experiments, we considered the GCO-500 phase of the mission. During this phase, the JUICE spacecraft will be in a nearly polar circular orbit around Ganymede at 500-km altitude (the real altitude ranges from 470 to 530 km). This part of the mission will last 130 days. The acquisitions of RIME are constrained by an important environmental factor. Indeed, Jupiter is a source of radio emissions, which can strongly interfere with the acquisitions and reduce the SNR of the acquired data, thus damaging their information content. For this reason, the acquisitions of RIME should be performed when the JUICE spacecraft is occulted by Ganymede with respect to Jupiter. Moreover, Ganymede is in *tidal locking* with Jupiter, meaning that its rotation period and its revolution period are almost the same. Thus, Ganymede always has the same side directed toward Jupiter. These conditions reduce the analysis to about a 30% of Ganymede's surface, which is still large.

The analysis of the RIME observation operations has been carried out using the proposed approach. The main requirements for the solution of this problem are the following.

1) To achieve uniform coverage of the surface of Ganymede in the investigated area.
2) To select segments of acquisition tracks spaced among each other of about 50 km.

A further guideline to take into account is to try to limit bursts of resources consumption, which may limit the acquisitions performed by the other instruments. Thus, an additional variable that has been considered in the definition of the scheduling is the daily duration of the acquisitions, with the objective to obtain an almost uniform distribution of this time in the full orbital phase.

B. Setup of Experiments

The first phase (segmentation) starts by taking as an input the trajectory that the spacecraft will perform during its orbit around Ganymede and the time span of the GCO-500 phase as our Φ. As explained in Section III, the trajectories are defined in a set of kernel files (those of the JUICE mission can be found at [24]) that contain the state vector (made of position and speed) of the satellite in time. For what concerns the JUICE mission, these files are defined by the Operation Center of ESA based on the Consolidated Reports on Mission Analysis. We consider the file reported in [25]. The input time interval Φ goes through the assessment of all the feasible observation opportunities: all the time intervals in which the acquisitions with RIME are not feasible are removed. These intervals correspond to instants in which the JUICE spacecraft is not shadowed from Jupiter by Ganymede, and thus, acquisitions might be affected by the interference produced by the Jovian electromagnetic noise. Moreover, the intervals related to the downlink windows (the information about them is also contained in one of the kernel files mentioned above) are removed. In these intervals, the ground segment (situated in Malargüe) is in line of sight with the satellite, and therefore, the resources of the satellite are dedicated to the transmission of the data. No acquisition is possible during these time windows. After the assessment of all the practical observation opportunities, we have a set Φ_f of time intervals, in which the acquisition with RIME is feasible. Accordingly, we identify the related positions on Ganymede's surface, obtaining the possible long acquisition tracks.

Considering the set of high-interest targets provided by the RIME Science Working Team on the analyzed area and subdividing the remaining surface in ten latitude bands (as shown in Fig. 3), we could split the acquisition tracks and the related time intervals, thus obtaining the set S of segments to use in the next phase. We also defined a set of uniformly distributed points $P = \{p_1, p_2, \ldots, p_M\}$ on the area over which acquisitions are feasible, which represent a quantization of the surface. Indeed, exploiting P, we can simplify the calculation of the covered surface, keeping also track of the coordinates of the points that are covered by each acquisition segment and of those that are not. We similarly defined a set $P_t \subset P$ that identifies the points on the surface included in the high-relevance areas. After the segmentation phase, we obtained a set S with more than 5000 segments. For each of them, we generated the influence areas $a(s_i)$ (whose width has been set at 50 km) and extracted data such as the number of points covered by each influence area $\{p_k \in a(s_i)\}$, the duration ($time(s_i)$) of the acquisition, and the day $day(s_i)$ in which the acquisition defined by each segment should be executed. We assumed that the acquisitions performed by RIME during the GCO-500 phase have a constant generated datarate (DR) and a constant power consumption (P_{acq}). Thus, we have $m(s_i) = DR \cdot time(s_i)$ and $e(s_i) = P_{\text{acq}} \cdot time(s_i)$. Therefore, we can easily analyze the resource consumption through the evaluation of the acquisition time.

We applied the proposed approach by using the NSGA-II algorithm. We expressed the quality metrics in terms of cost, i.e., better solutions correspond to smaller values of the metrics. Accordingly, the global metrics used for the evaluation of the solutions are defined as follows.

1) $unif(\mathbf{x})$: the track distribution uniformity, expressed as the percentage of points of the set P that are not covered one and only one time. We can formalize it as follows:

$$unif(\mathbf{x}) = \frac{|P| - L}{|P|} \tag{13a}$$

where

$$L = \sum_{j=1}^{|P|} h_j \tag{13b}$$

$$h_j = \begin{cases} 1, & \text{if } \sum_{i=1}^{N} k_{j,i} x_i = 1 \\ 0, & \text{otherwise} \end{cases} \tag{13c}$$

$$k_{j,i} = \begin{cases} 1, & \text{if } p_j \in a(s_i) \\ 0, & \text{otherwise} \end{cases} \tag{13d}$$

with $p_j \in P$.

2) $unif_t(\mathbf{x})$: the track distribution uniformity on areas of higher interest, expressed in a similar way as the previous metric, but focusing on the set P_t. We define it as follows:

$$unif_t(\mathbf{x}) = \frac{|P_t| - Q}{|P_t|} \tag{14a}$$

where

$$Q = \sum_{l=1}^{|P_t|} v_l \tag{14b}$$

$$v_l = \begin{cases} 1, & \text{if } \sum_{i=1}^{N} w_{l,i} x_i = 1 \\ 0, & \text{otherwise} \end{cases} \tag{14c}$$

$$w_{l,i} = \begin{cases} 1, & \text{if } p_l \in a(s_i) \\ 0, & \text{otherwise} \end{cases} \tag{14d}$$

with $p_l \in P_t$.

3) $\sigma(\mathbf{x})$: the uniformity in time of the acquisitions. This parameter allows us to distribute the acquisitions as evenly as possible on different days. It is possible to define it as follows:

$$\sigma(\mathbf{x}) = std[D(\mathbf{x})] = \sqrt{\frac{1}{N_{\text{days}} - 1} \sum\nolimits_{d=1}^{N_{\text{days}}} [dat_d(\mathbf{x}) - \mu(\mathbf{x}))^2]} \tag{15a}$$

where:

$$D(\mathbf{x}) = \{dat_1(\mathbf{x}), dat_2(\mathbf{x}), \ldots, dat_{N_{\text{days}}}(\mathbf{x})\} \tag{15b}$$

$$dat_d(\mathbf{x}) = \sum_{i=1}^{N} g_{d,i} time(s_i) \tag{15c}$$

$$g_{d,i} = \begin{cases} 1, & \text{if } x_i = 1 \text{ and } day(s_i) = d \\ 0, & \text{otherwise} \end{cases} \tag{15d}$$

$$\mu(\mathbf{x}) = \frac{1}{N_{\text{days}}} \sum_{d=1}^{N_{\text{days}}} dat_d(\mathbf{x}) \tag{15e}$$

with N_{days} being the total number of days.

The requirement on the intersection points between the acquisition tracks was not used in these tests because the considered orbit and the related acquisition tracks present very few intersection points.

C. Results

We carried out different tests by considering different configurations for the selection stage. For the first tests, we implemented the constraints in the proposed solution generation operators, mutation, and crossover. Thus, no unfeasible solutions are explicitly evaluated, limiting the search space, as explained in Section III. By associating each segment to one of the latitude bands or to one of the higher interest areas (the cells of the grid used to segment the acquisition opportunities), we defined a set of constraints on the number of segments for each of these areas, so that the uniformity requirement can be more easily achieved

$$\sum_{i=1}^{N} c_{j,i} x_i \leq b_j \tag{16}$$

where x_i is the ith component of the binary solution vector $\mathbf{x}$ (as shown in Fig. 4), $c_{j,i} = \{0, 1\}$ is in this case the weight associated with the ith segment and the jth constraint, while b_j expresses the value of the upper bound in terms of the number of chosen segments per area.

For the successive tests, we implemented the modified mutation operator (the guided mutation), without introducing the constraints defined before. The metrics used to guide the generation of new schedules/solutions are the ones described in Section III-B, i.e., $t(s_i)$ and $r(s_i)$.

Figs. 6–8 show some examples of the results of the tests obtained with the two described configurations. The circular area in Figs. 6(a) and 7(a) is the one that we considered for our analysis. The white edges identify both the high-interest areas on the investigated area on Ganymede and the other portions of the surface considered during the segmentation phase. The different colors show an example for a specific solution, for both test configurations, of how well and how uniformly the considered portion of surface is covered. Figs. 6(b) and 7(b) show instead the results in terms of daily acquisition time, while Figs. 6(c) and 7(c) summarize the characteristics of the considered solutions. Both test configurations considered a population size (the number of different solutions evaluated at each iteration) of 100 elements. They took about 3.5 days to reach 50 000 generations on a single computing cluster node (24 cores running at 2.4 GHz, 96 GB of RAM). The solutions displayed in Figs. 6 and 7 obtain very good scores especially in terms of spatial uniformity of the selected segments. Indeed, this is evident both from the graphical representation and from the solution feature summary: for the constrained optimization result, we obtain a total coverage of 94.41% of the total investigated area with just a 4.85% of "overcovered" surface. These metrics are even slightly better for the result of the optimization implementing the modified mutation operator: 94.7% coverage of the considered surface with 4.65% of overcovered surface. Very similar percentages of coverage have been obtained for what concerns the high-relevance areas. Interpreting these results in terms of spatial distribution, they mean that on more than 90% of the analyzed surface, we obtained the correct distribution of the ground tracks with the required distance. On the remaining portion of the surface, the selected tracks were either slightly too far (causing lack of coverage) or too near (causing the overlap of the considered influence areas and therefore overcoverage) from each other. Moreover, it is possible to see from Figs. 6(a) and 7(a) that these conditions are not concentrated in a particular region, but they are associated with very small regions distributed on the investigated area. This emphasizes the fact that the obtained results involve only a small irregularity in the spatial distribution of the selected segments, which is mostly due to the slight difference in the inclination of the available acquisition tracks.

The analysis of the daily acquisition time profiles for the two considered solutions also shows that the modified mutation was able to distribute the acquisition time more evenly, but both the analyzed solutions have obtained good and very similar values in terms of daily acquisition time standard deviation. These results should be interpreted considering the different daily constraints on the acquisition time in the time frame we are analyzing, which depend on the satellite orbit characteristics. Examples of Pareto

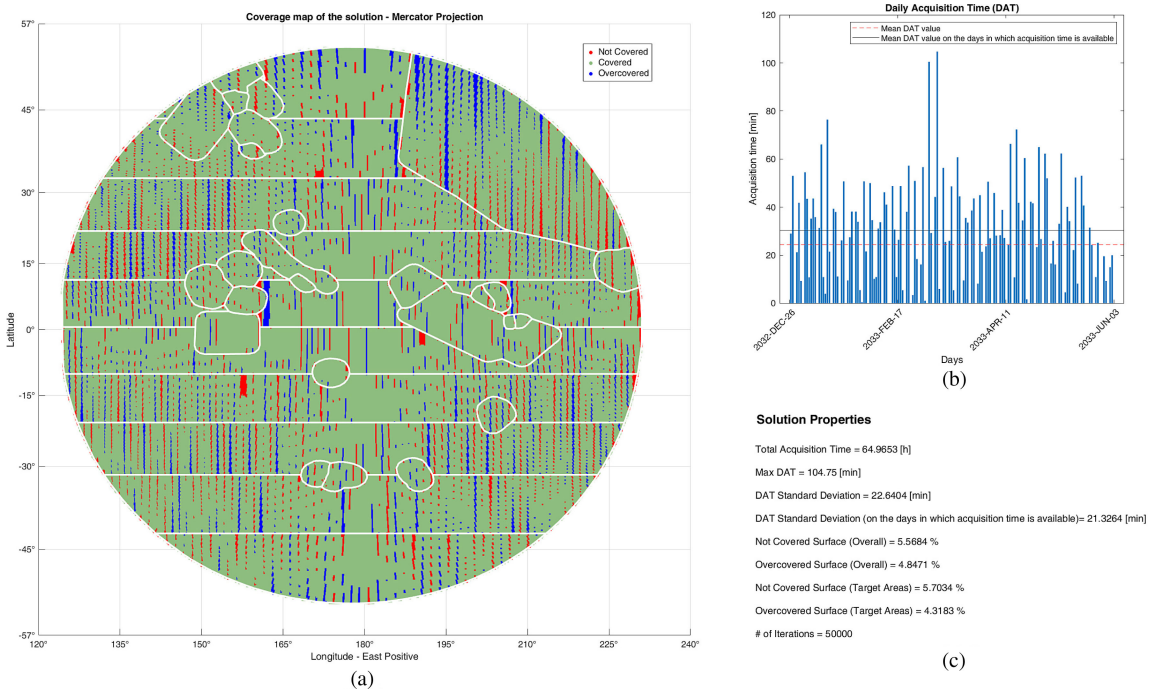

Fig. 6. Example of a solution of the multiobjective optimization achieved implementing the constraints on the number of segments to be active for each cell. This solution is the best in terms of spatial uniformity of the selected acquisition segments (GCO-500 case). The points that are covered by one and only one of the influence areas of the selected segments are in green. The points that are covered more than once are in blue. The points that are not covered are in red.

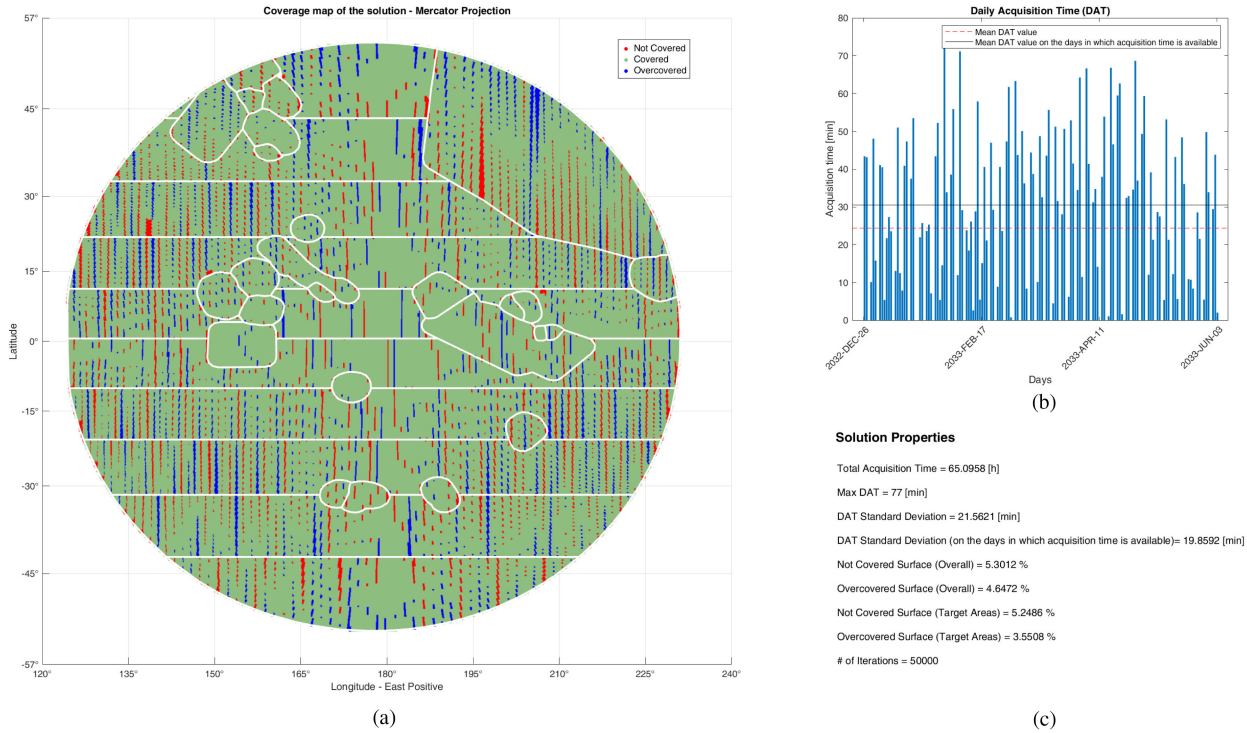

Fig. 7. Example of a solution of the multiobjective optimization achieved implementing the proposed mutation. This solution is the best in terms of spatial uniformity of the selected acquisition segments (GCO-500 case). The points that are covered by one and only one of the influence areas of the selected segments are in green. The points that are covered more than once are in blue. The points that are not covered are in red.

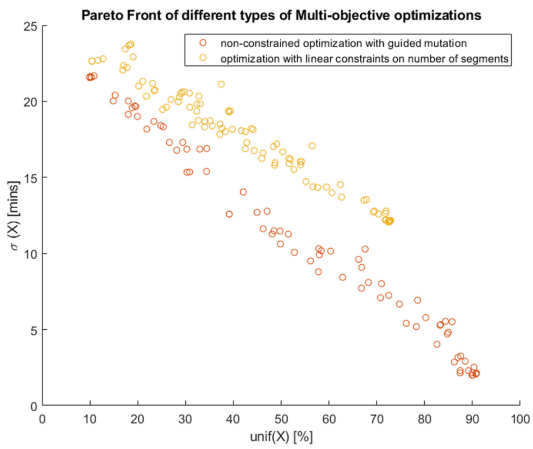

Fig. 8. Comparison of the two sets of solutions obtained after the selection phase with the implementation of the constraints on the number of segments per cell (in yellow) and with the guided mutation (in red). Here, one can see how different solutions are distributed, considering the two most important objectives of the experiment: $unif(X)$ and $\sigma(X)$. The solutions obtained with the second method are in general better as they dominate the solutions obtained with the first method.

fronts (i.e., the nondominated solutions of the multiobjective optimization) obtained with the two different optimization setups are reported in Fig. 8. These show the obtained solutions in terms of two of the considered objectives, i.e., $unif(\mathbf{x})$ and $\sigma(\mathbf{x})$. Part of these solutions do not show satisfactory results for the analyzed test case. In particular, this is the case of the ones on the right side of the two fronts. Nonetheless, the two sets of obtained solutions demonstrate that using a multiobjective technique, we can find a good number of candidate acquisition schedules related to multiple different optimal tradeoffs between the specified quality metrics describing the whole acquisition campaign. Moreover, the representation of the two Pareto fronts shows that the one obtained with the proposed guided mutation method is better than the one resulting from the configuration, in which we explicitly implemented the constraints on the number of acquisition segments to be selected for each cell. Indeed, all the solutions of the first front dominate the ones of the second front. This shows the efficiency of the proposed mutation operator for the exploration of the solution space and its potentiality in finding very good solutions for a large-dimensional problem.

VI. Conclusion

In this article, we have proposed an approach to the automation of the planning and scheduling process for planetary exploration missions. In particular, we have considered the study of acquisition operations of a single instrument included in the scientific payload of a mission. We have defined and presented an approach based on two main steps, segmentation and selection, showing its application to the particular case of radar sounder observations. For the segmentation phase, we defined a way to subdivide the long available acquisition time intervals into shorter segments based on a spatial criterion that allows the ground tracks not to be split over high-relevance targets. The resulting schedules are then produced in the selection phase, in which an optimized subset of the previously defined acquisition segment set is derived by using metrics that express the quality of the related acquisition schedule. For the selection phase, we considered two different configurations that use NSGAII-based multiobjective optimization techniques. The first configuration exploits the mission-specific and user-defined constraints to limit the otherwise very large search space. The second configuration, instead, implements a modified mutation operator, which performs a local search to more efficiently guide the exploration of the solution space toward high-quality solutions. We analyzed the proposed approach by considering its application to the real study case of the planetary radar sounder RIME on the JUICE mission. The obtained experimental results are very promising and show the potentialities of the proposed approach. From the achieved results, we can conclude that both configurations can produce high-quality solutions. With the first configuration, in fact, it was possible to efficiently limit the search space, avoiding nonsatisfactory solutions. With the second one, instead, we could reach a set of solutions that dominates the one obtained with the first configuration and, therefore, represents a collection of better tradeoffs of the considered objectives. This was obtained considering the same number of iterations and almost the same computational time. The results also show the importance of using a multiobjective technique, when multiple conflicting objectives are analyzed. Thus, the presented approach represents a good tool to produce optimized schedules for each instrument composing the scientific payload of a planetary exploration mission.

As future development of this work, we will consider to compare the results obtained by the proposed methodology with those achieved by methods used in EO missions. However, this requires a nonstraightforward adaptation of these methods to a planetary mission context. Moreover, the proposed approach is an interesting starting point for a global scheduling methodology that can consider multiple instruments at the same time. However, this results in an increase of the dimensionality of the problem in terms of the number of variables and the number of objectives and constraints to consider. This requires to further enhance the optimization strategy.

References

[1] P. Van Der Plas, B. García-Gutiérrez, F. Nespoli, and M. Pérez-Ayúcar, "MAPPS: A science planning tool supporting the ESA solar system missions," in *Proc. SpaceOps Conf.*, 2016, Art. no. AIAA 2016-2512.
[2] T. Choo *et al.*, "SciBox, an end-to-end automated science planning and commanding system," *Acta Astronautica*, vol. 93, pp. 490–496, 2014.
[3] K. Deb, A. Pratap, S. Agarwal, and T. Meyarivan, "A fast and elitist multiobjective genetic algorithm: NSGA-II," *IEEE Trans. Evol. Comput.*, vol. 6, no. 2, pp. 182–197, Apr. 2002.
[4] M. Ai-Chang *et al.*, "MAPGEN: Mixed-initiative planning and scheduling for the Mars Exploration Rover mission," *IEEE Intell. Syst.*, vol. 19, no. 1, pp. 8–12, Jan. 2004.
[5] H. Muraoka, R. Cohen, T. Ohno, and N. Doi, "ASTER observation scheduling algorithm," in *Proc. 5th Int. Symp. Space Mission Oper. Ground Data Syst.*, Tokyo, Japan, 1998.
[6] E. Maurer *et al.*, "TerraSAR-X mission planning system: Automated command generation for spacecraft operations," *IEEE Trans. Geosci. Remote Sens.*, vol. 48, no. 2, pp. 642–648, Feb. 2010.
[7] R. Knight and B. Smith, "Optimally solving nadir observation scheduling problems," in *Proc. 8th Int. Symp. Artif. Intell., Robot. Autom. Space*, Sep. 2005.

[8] G. Wu, H. Wang, W. Pedrycz, H. Li, and L. Wang, "Satellite observation scheduling with a novel adaptive simulated annealing algorithm and a dynamic task clustering strategy," *Comput. Ind. Eng.*, vol. 113, pp. 576–588, 2017.
[9] C. H. Acton, "Ancillary data services of NASA's Navigation and Ancillary Information Facility," *Planet. Space Sci.*, vol. 44, no. 1, pp. 65–70, 1996.
[10] C. Acton, N. Bachman, B. Semenov, and E. Wright, "A look towards the future in the handling of space science mission geometry," *Planet. Space Sci.*, vol. 150, pp. 9–12, 2018.
[11] J. Puchinger, G. Raidl, and U. Pferschy, "The multidimensional knapsack problem: Structure and algorithms," *INFORMS J. Comput.*, vol. 22, no. 2, pp. 576–588, Apr. 2010.
[12] M. Emmerich and A. Deutz, "A tutorial on multiobjective optimization: Fundamentals and evolutionary methods," *Natural Comput.*, vol. 17, no. 3, pp. 585–609, Sep. 2018.
[13] C. Persello and L. Bruzzone, "A novel protocol for accuracy assessment in classification of very high resolution images," *IEEE Trans. Geosci. Remote Sens.*, vol. 48, no. 3, pp. 1232–1244, Mar. 2010.
[14] L. Pasolli, C. Notarnicola, and L. Bruzzone, "Multi-objective parameter optimization in support vector regression: General formulation and application to the retrieval of soil moisture from remote sensing data," *IEEE J. Sel. Topics Appl. Earth Observ. Remote Sens.*, vol. 5, no. 5, pp. 1495–1508, Oct. 2012.
[15] F. Xhafa, J. Sun, A. Barolli, A. Biberaj, and L. Barolli, "Genetic algorithms for satellite scheduling problems," *Mobile Inf. Syst.*, vol. 8, pp. 351–377, Oct. 2012.
[16] V. Kolici, X. Herrero, F. Xhafa, and L. Barolli, "Local search and genetic algorithms for satellite scheduling problems," in *Proc. 8th Int. Conf. Broadband Wireless Comput., Commun. Appl.*, Oct. 2013, pp. 328–335.
[17] M. Lemaître, G. Verfaillie, F. Jouhaud, J. Lachiver, and N. Bataille, "Selecting and scheduling observations of agile satellites," *Aerosp. Sci. Technol.*, vol. 6, no. 5, pp. 367–381, 2002.
[18] L. Carrer and L. Bruzzone, "Solving for ambiguities in radar geophysical exploration of planetary bodies by mimicking bats echolocation," *Nature Commun.*, vol. 8, 2017, Art. no. 2248.
[19] R. Jordan *et al.*, "The Mars Express MARSIS sounder instrument," *Planet. Space Sci.*, vol. 57, no. 14, pp. 1975–1986, 2009.
[20] R. Croci, R. Seu, E. Flamini, and E. Russo, "The SHAllow RADar (SHARAD) onboard the NASA MRO Mission," *Proc. IEEE*, vol. 99, no. 5, pp. 794–807, May 2011.
[21] S. Paterna, L. Bruzzone, and M. Santoni, "An automatic planning and scheduling method based on multi-objective Genetic Algorithms for planetary radar sounder observations," in *Proc. IEEE Int. Geosci. Remote Sens. Symp.*, to be published.
[22] L. Bruzzone, G. Alberti, C. Catallo, A. Ferro, W. Kofman, and R. Orosei, "Subsurface radar sounding of the Jovian Moon Ganymede," *Proc. IEEE*, vol. 99, no. 5, pp. 837–857, May 2011.
[23] L. Bruzzone *et al.*, "Jupiter ICY moon explorer (JUICE): Advances in the design of the radar for Icy Moons (RIME)," in *Proc. IEEE Int. Geosci. Remote Sens. Symp.*, Jul. 2015, pp. 1257–1260.
[24] JUICE SPICE Kernels Set. [Online]. Available: https://www.cosmos.esa.int/web/spice/spice-for-juice. Accessed: Aug. 18, 2020.
[25] A. Boutonnet, J. Schoenmaekers, and W. Martens, "JUpiter Icy moons Explorer (JUICE): Consolidated report on mission analysis (CReMA)," Tech. Rep. ESA/SRE(2014)1 no. 3, Oct. 2015.

Stefano Paterna (Student Member, IEEE) received the "Laurea" (B.Sc.) degree in electronics and telecommunication engineering and the "Laurea Magistrale" (M.Sc.) degree in telecommunications engineering, in 2015 and 2017, respectively, from the University of Trento, Trento, Italy, where he is currently working toward the Ph.D. degree in information and communication technologies with the Remote Sensing Laboratory.

His research interests include the use of radar sounders for planetary exploration missions.

Massimo Santoni received the B.S. degree in electronics and telecommunication engineering and the M.S. degree in telecommunication from the University of Trento, Trento, Italy, in 2012 and 2014, respectively.

He is currently with the University of Trento, where he is working on the design of the Radar for Icy Moon Exploration instrument of the Jupiter Icy Moons Explorer mission of the European Space Agency. His research interests include the performance evaluation and design of radar sounder instruments and the study of the snow parameters using long time series of optical and synthetic aperture radar data.

Lorenzo Bruzzone (Fellow, IEEE) received the Laurea (M.S.) degree in electronic engineering (*summa cum laude*) and the Ph.D. degree in telecommunications from the University of Genoa, Genoa, Italy, in 1993 and 1998, respectively.

He is currently a Full Professor of Telecommunications with the University of Trento, Trento, Italy, where he teaches remote sensing, radar, and digital communications. He is the Founder and the Director of the Remote Sensing Laboratory, Department of Information Engineering and Computer Science, University of Trento. He is the Principal Investigator of many research projects. Among the others, he is currently the Principal Investigator of the Radar for Icy Moon Exploration instrument in the framework of the Jupiter Icy Moons Explorer mission of the European Space Agency (ESA) and the Science Lead for the High Resolution Land Cover project in the framework of the Climate Change Initiative of the ESA. He is the author (or coauthor) of 276 scientific publications in referred international journals (209 in IEEE journals), more than 330 papers in conference proceedings, and 22 book chapters. He is the Editor/Co-Editor of 18 books/conference proceedings and one scientific book. His papers are highly cited, as proven from the total number of citations (more than 34 000) and the value of the H-index (87) (source: Google Scholar). He was invited as keynote speaker in more than 40 international conferences and workshops. He promotes and supervises research on his research interests within the frameworks of many national and international projects. His current research interests include remote sensing, synthetic aperture radar, signal processing, machine learning, and pattern recognition.

Dr. Bruzzone has been a member of the Administrative Committee of the IEEE Geoscience and Remote Sensing Society (GRSS), since 2009. He has been the Vice-President for Professional Activities in IEEE GRSS, since 2019. He ranked first place in the Student Prize Paper Competition of the 1998 IEEE International Geoscience and Remote Sensing Symposium (IGARSS), Seattle, WA, USA, July 1998. He was the recipient of many international and national honors and awards, including the recent IEEE GRSS 2015 Outstanding Service Award, the 2017 and 2018 IEEE IGARSS Symposium Prize Paper Awards, and the 2019 WHISPER Outstanding Paper Award. He was a Guest Co-Editor of many Special Issues of international journals. He is the co-founder of the IEEE International Workshop on the Analysis of Multitemporal Remote-Sensing Images series and is currently a member of the Permanent Steering Committee of this series of workshops. Since 2003, he has been the Chair of the SPIE Conference on Image and Signal Processing for Remote Sensing. He is the Founder of the *IEEE Geoscience and Remote Sensing Magazine* for which he has been the Editor-in-Chief from 2013 to 2017. He is an Associate Editor for the IEEE TRANSACTIONS ON GEOSCIENCE AND REMOTE SENSING. He has been a Distinguished Speaker of the IEEE Geoscience and Remote Sensing Society from 2012 to 2016.